THE UNIVERSITY of EDINBURGH

Edinburgh Research Explorer

# Wave packet dynamics in the optimal superadiabatic approximation

OPEN ACCESS

# Wave packet dynamics in the optimal superadiabatic approximation

V. Betz,[1] B. D. Goddard,[2] and U. Manthe[3]

[1] *Fachbereich Mathematik, TU Darmstadt*

[2] *The School of Mathematics and Maxwell Institute for Mathematical Sciences,*
*University of Edinburgh*

[3] *Fakultät für Chemie, Universität Bielefeld*

We explain the concept of superadiabatic representations and show how in the context of electronically non-adiabatic transitions they lead to an explicit formula that can be used to predict transitions at avoided crossings. Based on this formula, we present a simple method for computing wave packet dynamics across avoided crossings. Only knowledge of the adiabatic potential energy surfaces near the avoided crossing is required for the computation. In particular, this means that no diabatization procedure is necessary, the adiabatic electronic energies can be computed on the fly, and they only need to be computed to higher accuracy when an avoided crossing is detected. We test the quality of our method on the paradigmatic example of photo-dissociation of NaI, finding very good agreement with results of exact wave packet calculations.

## I. INTRODUCTION

Superadiabatic approximations were first introduced by Michael Berry[1] in the context of a generalized Landau-Zener Hamiltonian. They can be viewed as iterative improvements to the adiabatic approximation, in the same spirit that higher order perturbation expansion improves first order perturbation theory. In the work of Berry a semiclassical approximation was made, and the nuclei were assumed to move classically. An extension of the theory to the full Born-Oppenheimer approximation has been done in recent years (see Refs 2–4). In this introduction we discuss the theory of superadiabatic approximations in the Born-Oppenheimer context on an intuitive level; mathematical details will be given later.

To understand superadiabatic approximations, consider first the adiabatic one. In the adiabatic representation, the frame of reference at each point in space is adjusted so that the electronic Hamiltonian is diagonal. In a time-dependent picture, the frame of reference thus 'moves with the nuclei', and it depends only on the position of the nuclei. By this procedure, the adiabatic representation achieves that, in most situations, a wave packet started on an adiabatic potential energy surface remains there to a very good approximation. The errors to this invariance property are described by the kinetic coupling element.

The superadiabatic representations improve on the adiabatic one by taking finer aspects (like, for example, the momentum) of the moving wave packet into account. The result is that the kinetic coupling from the adiabatic representation is transformed into a coupling depending on the second or higher derivatives of the nuclear wave function, but is now of much smaller magnitude. In many situations, already the quality of the adiabatic approximation is sufficient for describing the wave packet dynamics, and then there is no need for further improvements. In other cases, however, it is advantageous to go beyond the adiabatic approximation.

One of those situations are avoided crossings of potential energy surfaces. At an avoided crossing, the adiabatic derivative couplings become large (but do not diverge). Typically the relevant nuclear configurations are indicated by a very small, but finite, energetic distance of the corresponding adiabatic potential energy surfaces, whence the name 'avoided crossing'. As a result, a small but not negligible part of the nuclear wave packet traveling through the avoided crossing will make a transition to the previously unoccupied adiabatic energy surface.

While such a transition can still be described in the adiabatic representation, this leads to apparently complicated dynamics: when the wave packet approaches the avoided crossing, relatively large portions of it show up in the previously unoccupied adiabatic energy surface. This is illustrated in Figure 1, which shows the (exact) time evolution of the wave packet passing through an avoided crossing (for a NaI inspired system with a modified potential where $A_{12}$, see Section III for details, is increased to 0.08 eV) in the adiabatic representation. A wave packet initially located on the upper adiabatic potential energy surface approaches the avoided crossing and a wave packet on the lower adiabatic energy surface appears. Most of the wave packet on the lower adiabatic energy surface vanishes again after the passage of the avoided crossing but a much smaller second wave packet (marked red in the lower right panel of Figure 1 at t=209 fs and t=292 fs) emerges on the lower adiabatic surface at a different position and at a different momentum. The resulting effective non-adiabatic transition is described by that second wave packet, not the first one. The first wave packet only gives rise to temporary Stückelberg oscillations of the electronic populations during the passage of the avoided crossing. While in real world systems (at least for the example of NaI below) this effect is much less drastic than in the example presented in Fig.1, it is still present to some extent. This

FIG. 1. Snapshots illustrating the wave packet motion via an avoided crossing: The upper panel shows the adiabatic potential energy surfaces (black lines) and the wave packet $\psi_+$ on the upper adiabatic surface (snapshots at t=110 fs, t=176 fs, and t=209 fs are shown by red, blue, and green lines, respectively). Snapshots of the wave packet on the lower adiabatic potential energy surface are displayed on the lower panels in position ($\psi_-$) and momentum ($\hat{\psi}_-$) representation. In the first snapshots, the original wave packet approaches the transition point. A (spurious) wave packet starts to build up on the other adiabatic surface. At t=176 fs, the incoming wave packet is on top of the avoided crossing, and the spurious transmitted wave packet has grown to its maximal size. In the remaining snapshots, the incoming wave packet travels away from the avoided crossing, and the spurious wave packet starts to die down, revealing the much smaller true transmitted wave packet. This true transmitted wave packet is marked red when it becomes clearly visible in the momentum representation at times t=209 fs and 292 fs. In the final snapshot, the transition is over, and only the true transmitted wave packet remains.
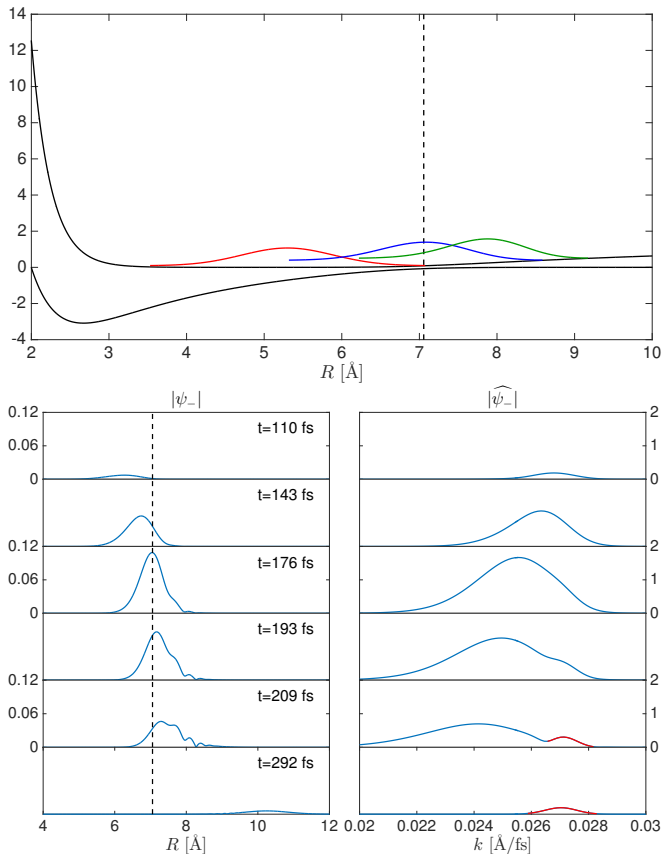


suggests that the adiabatic representation might not be the ideal frame of reference for understanding transitions at avoided crossings.

If we are only interested in the crossing probability, i.e. the expected population on the initially unoccupied adiabatic electronic state, we can use the Landau-Zener formula, which has been known for a long time[5] and also has a firm mathematical foundation[6]. In a nutshell, the Landau-Zener formula first applies a semiclassical approximation to the wave packet dynamics, and then avoids resolving the Stückelberg oscillations by deforming the time axis into the complex plane in the relevant region. What the Landau-Zener formula does not provide is information about the phase, or more generally any information about the transmitted wave packet except its size. This is where superadiabatic representations come into play.

Just like the *adiabatic* representation improves on the diabatic one by revealing the separation of nuclear dynamics according to electronic states, superadiabatic representations improve on the adiabatic one by giving a simpler dynamical picture in the vicinity of an avoided crossing. Observing the wave packet dynamics in higher and higher superadiabatic representations initially reduces the spurious oscillations in the wave packet dynamics, until the population on the previously unoccupied *superadiabatic* electronic state builds up monotonically as the wave packet travels through the avoided crossing: the Stückelberg oscillations have disappeared. The order of superadiabatic representation where this happens is called the optimal one. Going to even higher superadiabatic representations from that point on reveals the asymptotic nature of the superadiabatic expansion: in those representations the spurious transmitted wave packet starts to grow again and its size eventually diverges as the order of superadiabatic approximation goes to infinity.

The computation of the unitary operators leading to the superadiabatic representations, or of the optimal superadiabatic representation, is usually very difficult. However, it has been discovered[2,3] that it is possible to give an explicit formula for the transmitted wave packet in the optimal superadiabatic representation without knowing the unitary transformation leading to it. By general theory[7], all superadiabatic representations agree with the adiabatic one away from an avoided crossing with very good accuracy. This leads to a straightforward algorithm for efficiently computing transitions across avoided crossings, which has been shown to perform well in model systems[3].

The present work investigates the prospects of the superadiabatic theory for the description of realistic molecular systems. A simple but prototypical example, the photodissociation of NaI induced by a femtosecond laser pulse, is studied. All aspects related to the detailed description of the non-adiabatic transitions within the superadiabatic representation are discussed and addressed. Comparisons with accurate wave packet dynamics calculations demonstrate the accuracy of the superadiabatic theory. Furthermore, different approximations connecting the superadiabatic wave packet propagation with semi-classical calculations based on Landau-Zener formulas are discussed and their accuracy is studied numerically.

The paper is organized as follows. In section II, we outline the theory of superadiabatic representations and

explain how they lead to a rather explicit formula for non-adiabatic transitions. We also describe how this formula is used for a straightforward numerical scheme for computing transitions. In section III, we describe the NaI system quantitatively and give the numerical details of our algorithm. Finally, we state the results.

## II. THEORY

### A. Superadiabatic approximations

In practice, the natural starting point for superadiabatic approximations is the adiabatic one. For explaining the nature of superadiabatic representations it is of advantage to start with the diabatic representations and recall how it relates to the adiabatic representation. We will not discuss the subtle issues of diabatization and existence of a diabatic representation[8]. Instead, we just assume that we start with a molecular system with one nuclear degree of freedom and two electronic states. A diabatic representation has the property that there are no derivative couplings, and so the Hamiltonian of the system must have the form

$$H = -\frac{\varepsilon^2}{2}\partial_R^2 \boldsymbol{I} + V(R), \text{ with } V(R) = \begin{pmatrix} V_{11}(R) & V_{12}(R) \\ V_{21}(R) & V_{22}(R). \end{pmatrix} \quad (1)$$

Here $\boldsymbol{I}$ is the $2 \times 2$ identity matrix, and $\varepsilon^2$ is the 'inverse reduced mass'. It will turn out that we need to know the numerical value of $\varepsilon$ accurately for computing quantitatively correct transition wave packets. For a di-atomic molecule with nuclear masses $m_A$ and $m_B$ (measured in atomic mass units), we find that in units of [eV Å$^2$],

$$\varepsilon^2 \approx 4.18 * 10^{-3} \frac{m_A + m_B}{m_A m_B}. \quad (2)$$

For typical molecules (like NaI) we obtain values of approximately $10^{-4}$ for $\varepsilon^2$.

Solutions of the time dependent Schrödinger equation

$$i\hbar\partial_t\psi = H\psi \quad (3)$$

are $\mathbb{C}^2$-valued functions $\psi$ of the nuclear separation variable $R$. The diabatic representation allows for a straightforward application of standard wave packet dynamics methods and is well suited to describe the interaction between the system and the electromagnetic field. However, the molecular dynamics can frequently be more easily interpreted using the adiabatic representation (see, e.g., Ref. 9 for a detailed comparison of wave packet dynamics in diabatic and adiabatic representations). Non-adiabatic couplings tend to be much more localized than non-diabatic ones. Consequently, in the adiabatic representation the wave packet motion on the different potential energy surfaces is decoupled most of the time. Significant non-adiabatic couplings are only found when the

wave packet is close to an avoided crossing (or a conical intersection).

Superadiabatic representations are a systematic way to find further improved frames of references that give a simpler description of molecular dynamics near an avoided crossing. For describing them, we first transform to the adiabatic representation: for each $R$, let $U_0(R)$ be the unitary $2\times2$ matrix that diagonalizes $V(R)$. Then the $\mathbb{C}^2$-valued adiabatic wave function $\psi_0(R,t) = U_0(R)\psi(R,t)$ is the solution of the Schrödinger equation

$$i\hbar\partial_t\psi_0 = H_0\psi_0, \quad (4)$$

where $H_0 = U_0^{-1}HU_0$, or more explicitly

$$H_0 = -\frac{\varepsilon^2}{2}\partial_R^2 I + \begin{pmatrix} V_0^+(R) & -\varepsilon\kappa_1(R)(\varepsilon\partial_R) \\ \varepsilon\kappa_1(R)(\varepsilon\partial_R) & V_0^-(R) \end{pmatrix} + \mathcal{O}(\varepsilon^2). \quad (5)$$

Here, $\mathcal{O}(\varepsilon^2)$ signifies that there are further terms with a prefactor of $\varepsilon^2$. These are of no importance, since we will see shortly that the operator $\varepsilon\partial_R$ is in fact of order one. $V_0^+$ and $V_0^-$ are the upper (lower) adiabatic potential energy surfaces (the eigenvalues of the matrix $V$). The coefficients $\pm\kappa_1(R)$ of the first order differential operators on the off-diagonal are known as the adiabatic coupling elements and give the size of the derivative couplings. Overall, transitions are of order $\varepsilon$ (thus small), and the components $\psi_0^+$ and $\psi_0^-$ evolve approximately independently; but in the vicinity of an avoided crossing, $\kappa_1(R)$ becomes large, and the approximation of independence deteriorates. Non-adiabatic transitions are the result.

Starting from the representation (5), the idea of the first superadiabatic representation is now rather straightforward. We want to find another unitary operator $U_1 = U_0\tilde{U}_1$ so that the off-diagonal elements in

$$H_1 = U_1^{-1}HU_1 = \tilde{U}_1^{-1}H_0\tilde{U}_1$$

are even smaller than those of $H_0$. We can make this statement more precise using powers of $\varepsilon$, but for this it is necessary to first rescale time in such a way that the speed of the nuclei in the new units is independent of the value of $\varepsilon$. Rescaling time by a factor of $\hbar/\varepsilon$ transforms (4) into

$$i\varepsilon\partial_t\psi_0 = H_0\psi_0, \quad (6)$$

while leaving $H_0$ unchanged. In the new time scale, nuclear wave functions oscillate with a frequency of the order $\varepsilon^{-1}$, so as announced above, applying a derivative coupling of the form $\varepsilon^2\kappa_1^\pm(R)\partial_R$ actually produces a term of order $\varepsilon$ instead of $\varepsilon^2$.

We can now be more precise about the statement that in the first superadiabatic representation, the off-diagonal elements should be smaller: we require them to be (possibly higher order) polynomials in $\varepsilon\partial_R$ with a global prefactor of at most $\varepsilon^2$.

A systematic way to achieve this for all orders of $\varepsilon$ has been found in Ref. 2. There, unitary operators $U_n$ are constructed such that the $n$-th superadiabatic Hamiltonian $H_n = U_n^{-1}HU_n$ has the following properties:

- The diagonal elements of $H_n$ are the same as those of $H_0$, up to corrections that are of order $\varepsilon^2$. In other words, the dynamics inside a given electronic state is the adiabatic one.

- The off-diagonal elements of $H_n$ are $(n+1)$-th order polynomials in $\varepsilon\partial_R$ with $R$-dependent coefficients, and carry a global prefactor of $\varepsilon^{n+1}$.

- The off-diagonal elements of $H_{n+1}$ can be constructed from those of $H_k$, $k \leqslant n$ by solving a set of ordinary differential equations, see Proposition 3.3 of Ref. 2. It is here that the restriction to one-dimensional systems appears: for multiple degrees of freedom, a set of *partial* differential equations can be written down which recursively determines the $H_n$. However, we currently do not understand the behavior of the solutions to these equations well enough to analyze them asymptotically, i.e. we do not have an equivalent of equation (14) below.

Thus the Hamiltonian in the $n$-the superadiabatic representation reads, to leading order in $\varepsilon$:

$$H_n = -\frac{\varepsilon^2}{2}\partial_R^2 \boldsymbol{I} + \begin{pmatrix} V_0^+(R) & \varepsilon^{n+1}K_{n+1}^+ \\ \varepsilon^{n+1}K_{n+1}^- & V_0^-(R) \end{pmatrix}, \quad (7)$$

where the *$n$-th superadiabatic coupling element* $K_{n+1}^\pm$ is a polynomial in $\varepsilon\partial_R$ with coefficients depending on $R$. The computation of this polynomial is not trivial, e.g. since $\partial_Q$ and functions of $Q$ do not commute and an order problem needs to be solved. This can be done[2] using symbolic calculus and Weyl quantization.

The molecular wave function $\psi_n(t) = U_n\psi(t)$ in the $n$-th superadiabatic representation in rescaled time is then the solution of the of the Schrödinger equation in the $n$-th superadiabatic representation

$$i\varepsilon\partial_t\psi_n = H_n\psi_n. \quad (8)$$

If we choose the initial condition to be confined in one electronic state,

$$\psi_n(0) = \begin{pmatrix} \psi_n^+(0) \\ \psi_n^-(0) \end{pmatrix} = \begin{pmatrix} \phi \\ 0 \end{pmatrix},$$

then first order perturbation theory describes the transitions to the initially unoccupied electronic state: to leading order in $\varepsilon$, the second component $\psi_n^-(t)$ of $\psi_n(t) = U_n\psi(t)$ is given by

$$\psi_n^-(t) = -i\varepsilon^n \int_0^t e^{-(i/\varepsilon)(t-s)H^-} K_{n+1}^- e^{-(i/\varepsilon)sH^+} \phi \, ds, \quad (9)$$

where $H^\pm = -\frac{\varepsilon^2}{2}\partial_R^2 + V_0^\pm$ are the adiabatic Hamiltonians for the respective electronic states.

At this point we should remember that while $\varepsilon$ is a small number, it is fixed for a given molecular system and is not taken to zero. This means that we have no

guarantee that by switching to higher and higher superadiabatic representations, the off-diagonal elements of $H_n$ decrease. The reason is that the convergence of $\varepsilon^{n+1}$ to zero as $n \to \infty$ is offset by a very fast growth of the coefficients of the polynomials $K_{n+1}$. In Ref. 2 it is shown that as functions of $R$, these coefficients are maximal at points $R_c$ close to where the adiabatic potential energy surfaces exhibit an avoided crossing, and that as functions of $n$ the products $\varepsilon^n K_n^\pm$ first decrease until they become minimal at some $n_{\text{opt}}$, after which they start to increase and eventually diverge. $n_{\text{opt}}$ depends on the difference of adiabatic potential energy surfaces at $R_c$ and can be characterized by the property that the norm of the wave function $\psi_n^-(t)$ (9) builds up monotonically as the wave packet travels past the avoided crossing until it reaches the final value predicted by the Landau-Zener formula. In other words $n_{\text{opt}}$ is the representation where the Stückelberg oscillations have disappeared.

Superadiabatic unitary operators $U_n$ are very complicated objects. While the adiabatic unitary $U_0$ is just a rotation of configuration space (and thus easy to understand and to implement on a computer), or $n \geqslant 1$, the $U_n$ are pseudodifferential operators acting on the full wave function $\psi$. The complicated nature of these transformations is not surprising: in the same way as the adiabatic representation clings to the moving frame of reference given by the adiabatic electronic states, the superadiabatic representations try to cling to the complicated behavior observed during a non-adiabatic transition in order to represent it in a simple form; but then the dynamical complexity of the transition must be hidden in the transformation itself.

For the practitioner, this will cast serious doubts on the practical value of superadiabatic representations. For example, if equation (9) is to be of any practical use, one would first need to transform the initial condition (which will be given in the adiabatic representation) to the $n$-th superadiabatic representation, which is numerically hopeless. Additionally, any statement about the time-evolved wave function obtained from (9) would need to be transformed back to the adiabatic representation. So, equation (9) describes a possibly simple dynamics in a very complicated frame of reference, which is useless without a way of translating it back to a frame of reference that we can understand.

These objections are valid if we try to understand the adiabatic behavior of the molecular wave function at the precise time when it travels through the avoided crossing. But often we are more interested in the wave function at a time when it has already left the vicinity of the avoided crossing. In this case, we can make use of a convenient property of the superadiabatic representations[2]: when the support of a wave packet $\psi$ has no meaningful overlap with the region where an avoided crossing is located, the adiabatic representation and all superadiabatic representations agree with very high accuracy, in other words $U_n\psi \approx U_0\psi$ for such wave functions. This enables us to 'bypass' the difficulties of the adiabatic representation

during the non-adiabatic transition event in the following way:

1. While the wave packet is still located well away from the avoided crossing, we switch from the adiabatic to the optimal superadiabatic representation. These two representations agree, therefore no change to the wave packet is made.

2. We then follow the dynamics of the wave packet across the avoided crossing in the optimal superadiabatic representation. These dynamics will be simpler than the adiabatic ones, but we have no easy way of translating them back to the adiabatic representation while the wave packet is located near the avoided crossing. Nevertheless, the wave packet in the optimal superadiabatic representation will split up into two wave packets, each on one of the superadiabatic subspaces.

3. We follow the dynamics of both of these wave packets until their support is well away from the avoided crossing, then switch back to the adiabatic representation. The two representations agree, so no change to the wave packet is made.

In practice, this means that we can just use equation (9) all the way, where $\phi$ is the initial condition in the *adiabatic* representation. Likewise, $\psi_n^-$ is the transmitted wave packet in the *adiabatic* representation except when its center is very close to the avoided crossing.

**B.  Non-adiabatic transitions**

While we have now established that solving (8) is useful for studying the dynamics of non-adiabatic transitions, we still have to find an efficient way to actually solve it. More precisely, we need to compute the optimal superadiabatic coupling elements $K_{n_{\mathrm{opt}}}^{\pm}$ and the integral (9). This can be done with the help of asymptotics beyond all orders: it turns out[2,3] that $K_{n_{\mathrm{opt}}}^{\pm}$ has a universal, simple description which depends on very few parameters of the model. We review the main arguments and the result here and refer to the cited references for details.

The relevant quantity that completely determines the non-adiabatic transition is the energy difference of the adiabatic potential energy surfaces in the vicinity of the avoided crossing. Since the adiabatic potential energy surfaces $V_\pm$ do not quite cross, we can order them so that $V_+(R) > V_-(R)$ for all relevant $R$. We define

$$\rho(R) = \tfrac{1}{2}\big(V_+(R) - V_-(R)\big) > 0, \qquad (10)$$

and observe that when the avoided crossing is at $R = R_c$, then by definition $\rho$ has a local minimum there.

From the work of Berry and Lim[10] it is possible to derive a nonlinear rescaling of the nuclear configuration space in which the *adiabatic* coupling elements obtain a universal shape. We define the *natural scale* by

$$\tau(R) = 2 \int_{R_{\mathrm{c}}}^{R} \rho(r)\, \mathrm{d}r, \qquad (11)$$

and extend the function $\rho$ and $\tau$ into the complex plane. By the theory of Stokes lines[6], the analytic continuation of $\rho$ has a pair of complex conjugate zeros at locations $R_{\mathrm{cz}}$ and $R_{\mathrm{cz}}^*$ close to $R_c$. Let

$$\tau_{\mathrm{c}} = \tau(R_{\mathrm{cz}}). \qquad (12)$$

Near $R = R_{\mathrm{c}}$, the adiabatic coupling elements are of the universal form

$$\kappa_1(R) = \frac{\mathrm{i}\rho(R)}{3}\Big[\Big(\frac{1}{\tau(R)-\tau_{\mathrm{c}}^*} - \frac{1}{\tau(R)-\tau_{\mathrm{c}}}\Big) + \kappa_{\mathrm{r}}(\tau(R))\Big], \qquad (13)$$

where the remainder term $\kappa_{\mathrm{r}}$ has singularities of order strictly less than 1 at the points $\tau_c = \tau(R_{\mathrm{cz}})$ and $\tau_c^* = \tau(R_{\mathrm{cz}}^*)$.

Universality of the optimal superadiabatic coupling elements follows from (13) by the Darboux principle[11,12], which guarantees that in the recursion for computing the superadiabatic representations[2], the dominant contribution to $K_{n+1}^{\pm}$ stems from taking derivatives (with respect to $R$) of $K_n^{\pm}$. The shape of high derivatives of meromorphic functions is dominated by the highest order complex singularities nearby[13], which means that the remainder terms in (13) play no role. We define

$$h_n(\tau) = \frac{\mathrm{i}}{(\tau - \tau_{\mathrm{c}}^*)^n} - \frac{\mathrm{i}}{(\tau - \tau_{\mathrm{c}})^n},$$

and

$$\kappa_n^-(R) = (n-1)!\,\rho(R)\frac{\mathrm{i}^n}{\pi}h_n(\tau(R)).$$

The dominant contribution to $K_{n+1}^-$ is then given[3] by the fully symmetrized operator product of $\mathrm{i}\varepsilon\partial_R$ with the multiplication operator $\kappa_{n+1}^-$:

$$K_{n+1}^-\phi = \sum_{j=0}^{n+1}\binom{n+1}{j}\Big(\frac{\varepsilon}{2\mathrm{i}}\Big)^j\big(\partial^j\kappa_{n+1}^-\big)(-\mathrm{i}\varepsilon\partial_R)^{n+1-j}\phi. \qquad (14)$$

Here, $\partial^j\kappa_{n+1}^-$ is the $j$-th derivative of $\kappa_{n+1}^-$ with respect to $R$.

Formula (14) shows that the operator $K_{n+1}^-$ is strongly spatially localized: Since $\kappa_{n+1}^-$ and all its derivatives are rapidly decaying away from $R_{\mathrm{c}}$, $K_{n+1}^-\phi = 0$ for a wave packet $\phi$ with support not overlapping a small vicinity of $R_{\mathrm{c}}$. While even the adiabatic coupling element $K_1^-$ exhibits some of this localization, this effect becomes much stronger as we increase $n$.

For the optimal superadiabatic representation, this concentration is strongest, and non-superadiabatic transitions happen much more quickly than in the non-adiabatic ones. In equation (9), the consequence is that

the integral only has to be evaluated for values of $s$ that are very close to the time $s_c$ where the center of the wave packet $e^{-(i/\varepsilon)sH^+}\phi$ is at $R_c$. This is exploited in Ref. 3: since the integration time in (9) is so short, the nuclear dynamics *on* both of the adiabatic energy surfaces can be replaced by quantum dynamics in the linear approximation of the adiabatic potentials, for which there is an analytic formula. The asymptotic form of $\kappa_{n_{\mathrm{opt}}}^-$ can be analyzed, and then $\psi_n$ in (9) can be expressed by an explicit integral formula (see equation (10) of Ref. 3) which is still complicated but no longer contains any propagators. It is analyzed further in Ref. 4.

In many situations, the time it takes the wave packet to travel through the crossing region is so short that a further simplification gives sufficiently good results: we use free propagation for the adiabatic dynamics near the avoided crossing in formula (9) instead of approximating the adiabatic potential energy surfaces by linear ones. Then another dramatic simplification takes place[3]. Let $\psi_0^+(R, t_c)$ be the upper adiabatic component of the wave packet, at the time $t_c$ when its center arrives at $R_c$. Then for $t > t_c$, the expression (9) can be approximated by

$$\psi_n(R, t) = e^{-(i/\varepsilon)(t-t_c)H^-}\psi^-(R),\qquad(15)$$

where $\psi^-(R)$ is a wave packet instantaneously created at time $t_c$, and having Fourier transform

$$\widehat{\psi}^-(k) = -\Theta(k^2 - 4\delta)\frac{v+k}{2|v|}e^{i\tau_c|k-v|/(2\delta\varepsilon)}\hat{\psi}_0^+(v, t_c)\ (16)$$

Here, $\delta = \rho(R_c)$ is half the energy gap at the avoided crossing, and $k$ is the momentum variable. $\Theta$ is the Heaviside function. The Fourier transform needs to be done in the correct scale involving $\varepsilon$, i.e.

$$\hat{\psi}(k) = \frac{1}{\sqrt{2\pi\varepsilon}}\int e^{-(i/\varepsilon)kR}\psi(R)\,dR.\qquad(17)$$

Finally, $v = v(k, \delta) = \mathrm{sgn}(k)\sqrt{k^2 - 4\delta}$ is the initial momentum that a classical particle would need to have to end up with momentum $k$ after falling down a potential energy difference of $2\delta$. The Heaviside function enforces that no smaller momenta appear and that $v$ cannot become complex valued.

A few comments about formula (16) are in order:
1. The global sign in any formula relating the two adiabatic subspaces must be indefinite, due to the arbitrariness when choosing the sign of the eigenvectors in the adiabatic representation. Here we choose the sign to match the given adiabatic representation of our the NaI model below, in order to compare with exact dynamics. In Ref. 3, a different sign was used.
2. In NaI, the non-adiabatic transition is from the upper to the lower surface, and our formula (16) reflects that. It turns out (see in particular the derivation of formula (4.11) in Ref. 2), that a very similar formula describes the reverse transitions. If the wave packet is initially in the

lower superadiabatic state, the non-adiabatic transition to the upper superadiabatic state is given by

$$\widehat{\psi}^+(k) = -\frac{\tilde{v}+k}{2|\tilde{v}|}e^{i\tau_c|k-\tilde{v}|/(2\delta\varepsilon)}\hat{\psi}_0^-(\tilde{v}, t_c),\qquad(18)$$

with $\tilde{v}(k, \delta) = \mathrm{sgn}(k)\sqrt{k^2 + 4\delta}$ again being the momentum that a classical particle would need to end up with momentum $k$ after *jumping up* a potential energy of $2\delta$. Note that (18) predicts that energetically forbidden transitions do not happen: the values of $\hat{\psi}_0^-(k)$ with $|k| < 2\delta$ do not play any role in the computation of $\hat{\psi}^+$.
3. Even though formula (16) describes the evolution of the transmitted wave packet in the optimal superadiabatic representation, it does not depend on the value of $n_{\mathrm{opt}}$. This is a consequence of the asymptotic universality properties mentioned above.
4. Only local information about the adiabatic electronic energies near the avoided crossing is used: precisely, what is needed is the size of the gap $2\delta$ and the quantity $\tau_c$ given in equation (12).
5. Formula (16) has an obvious algorithmic interpretation, which we will give and use at the beginning of the next subsection.

A very useful way to think about (16) is to view it as a 'local in momentum' refinement of the classical Landau-Zener formula. For this, assume that $\delta$ is very small, i.e. the crossing of potential energy surfaces is very narrowly avoided. An expansion in $\delta$ then gives $|v(k)| \approx |k| - 2\delta/|k|$. Thus in (16), we can write $(v+k)/2v \approx k/|k|$, and $|k-v| \approx 2\delta/|k|$. For an approximate calculation of $\tau_c$ as given in (12), we can note that $\rho(R_c) = \delta$, and so the zeros of its analytic continuation are very close to the real line. In view of (11) an expansion in $(R - R_c)$ seems appropriate.

However, a naïve second order expansion of $\rho(R)$ around $R_c$ would give the wrong result. The reason is that, as has been noticed long ago[10], the analytic continuation of $\rho$ must vanish *like a square root* at its complex zeroes. The appropriate expansion is thus

$$\rho(R) \approx \sqrt{\delta^2 + g(R - R_c)},\qquad(19)$$

with smooth $g$ and $g(0) = g'(0) = 0$, and we have to do the second order expansion of $g$. This gives $\rho(R) \approx \sqrt{\delta^2 + \alpha^2(R - R_c)^2}$ with $\alpha^2 = \frac{1}{2}g''(0)$. With this form of $\rho$ both $R_{cz}$ and $\tau_c$ can be computed analytically. The result is

$$\tau_c \approx i\frac{\pi\delta^2}{2\alpha}.\qquad(20)$$

The connection with $\rho''(R_c)$ is made by twice differentiating (19) and comparing, and we find $\alpha = \sqrt{\delta\rho''(R_c)}$. The final result is that for small $\delta$, formula (16) is well approximated by

$$\widehat{\psi}^-(k) = -\frac{k}{|k|}\Theta(k^2-4\delta)e^{-\frac{\pi}{2\varepsilon}\frac{\delta^{3/2}}{|k|(\rho''(R_c))^{1/2}}}\hat{\psi}_0^+(v, t_c)\ (21)$$

A very similar formula appears as equation (4) in the paper[14] of Belyaev, Lasser and Trigila, where it gives the Landau-Zener transition rate for single switch surface hopping. The factor $|k|$ in the denominator of the exponent is present in our formula but not in theirs. The reason is that in the formula of Belyaev et al., the second derivative of $\rho$ is taken with respect to a point particle traveling on the adiabatic surface, while in our formula it is the curvature of the surface itself. Thus if we take $|k|$ as the speed of the point particle, the additional factor appears by the chain rule.

For small $\delta$, an application of (21) can thus be understood as an execution of the following steps:

1. decompose the wave function into plane waves of fixed momentum $k$,

2. perform a momentum shift dictated by energy conservation (this is the significance of the argument $v$ in $\widehat{\psi}^+$).

3. compute the single switch surface hopping Landau-Zener probability $P_k$ for a point particle with momentum $k$,

4. put the fraction $P_k$ of the wave packet at momentum $k$ on the other adiabatic surface.

5. reassemble the wave function from the $k$-slices obtained above.

An application of the actual formula (16) can be understood in a similar way, but where in step 3 we apply a more refined transition probability which does not rely on $\delta$ being very small.

There is, however, a very significant difference between (21) and a surface hopping formula, which comes from the expression $k/|k|$. It indicates that the direction in which the original wave packet traverses the avoided crossing matters and contributes an overall sign to the transmitted wave packet. While for single transitions, this is insignificant, it matters greatly when two of these generated wave packets interfere. In Section IV we will see that for the example of NaI, this is indeed the case.

### C. Implementation

Here we present a simple algorithm for computing non-adiabatic transitions using formula (15). As we just discussed, there are conceptual similarities to surface hopping[14]. When compared to those methods, ours has the advantage of preserving phase information of the wave packet. Thus, the present method can correctly capture interference effects.

Our algorithm assumes that we have a way of propagating wave packets on uncoupled adiabatic potential energy surfaces, and a way to compute the adiabatic energy surfaces to reasonable accuracy in special regions, possibly on the fly. It then determines transitions between the superadiabatic electronic states as follows:

1. We propagate the adiabatic components $\psi_0^\pm$ of the wave packet on their respective adiabatic surfaces, with no coupling between the adiabatic potential energy surfaces. Any propagator can be used.

2. During the evolution, we monitor the distance $h(t) := V_0^+(t) - V_0^-(t)$ of the electronic energy surfaces at the center of all relevant wave packets.

3. When a minimum of $h(t)$ is detected for a wave packet, we estimate the size of the expected transition by using the classical Landau-Zener formula. If the estimated size is larger than a user-defined threshold, we

   (a) Go back to the point in time when the center was at the location $R_c$ of the avoided crossing.

   (b) Determine $\delta$ and $\tau_c$ from the adiabatic energy surfaces.

   (c) Put a wave packet according to (15) on the other electronic state.

4. Go back to step 1.

The numerical costs of the algorithm are essentially identical to the costs of a wave packet propagation on uncoupled potential energy surfaces. More importantly, its quality is not compromised when the desired output is a small quantity. The relative error of the transmitted wave packet is equal to the relative error of the single state propagator, plus systematic errors that reflect the approximate nature of formula (15).

There are two more comments to make about the algorithm. The first concerns the calculation of $\tau_c$ given in (12). At first sight, it seems that we need to compute the analytic continuation of the quantity $\rho$ which may not be known to a very high precision in practice. Fortunately, since non-adiabatic transitions are going to be negligibly small unless the adiabatic energy gap $\delta$ is small, we can use the approximation of $\rho$ given in (19), and thus use (20) instead of the true $\tau_c$. This way, we only need to know the second derivatives of the adiabatic potential energy surfaces at the point $R_c$ of the avoided crossing. Note, however, that the quantity $\pi/(2\varepsilon)$ that multiplies our approximation in (21) is usually rather large. To make things worse, the transition probability is obtained by exponentiating, potentially magnifying any errors we make. So it is not clear in all cases how good of an approximation (21) is. Below, we investigate the situation for the example of NaI, and find that the approximate formula is acceptable. In other situations, it may be necessary to find better approximations to $\rho(R - R_c)$ for good accuracy. On the other hand, a sufficiently detailed knowledge of the adiabatic potential energy surfaces is anyway a theoretical prerequisite to any meaningful prediction of non-adiabatic transitions.

The second comment is about slicing the wave function. Formula (15) evaluates the initial wave packet $\psi_0^+(R, t_c)$ at the time when its centre is on the crossing

point. In the derivation of that formula, it is assumed that $\psi_0^+$ is localized on the semiclassical scale matching the adiabatic propagators in (9). In other words, we need to assume that the width of $\psi_0^+$ is not much larger than $\sqrt{\varepsilon}$. In practice, this condition may be violated, and in fact this is what happens in the case of NaI below. There, we find that $\psi_0^+(R, t_c)$ is significantly different from zero on an interval of length about 2Å, or approximately $16\sqrt{\varepsilon}$. Here, a straightforward application of formula (16) would result in a poor accuracy. The solution is a slicing of the original wave packet. One can e.g. use a partition of unity, i.e. take compactly supported functions $g_1, \ldots, g_n$ with $\sum_{j=1}^n g_n(R) = 1$ for all $R$, and define $\psi_{0,j}^+(R) = g_j \psi_0^+(R, t_c)$. The width of each $g_j$ should be around $\sqrt{\varepsilon}$.

Each wave packet $\psi_{0,j}^+$ is then evolved on the upper adiabatic surface for the (possibly negative) time $t_j$ it takes for its center to reach $R_c$, where formula (15) is applied to it. This leads to a transmitted wave packet $\psi_j^-$ which is then evolved for the time $-t_j$ on the lower energy surface. All of these re-evolved $\psi_j^-$ are then summed up to produce the transmitted wave packet at time $t_c$.

Note that when the $g_j$ are chosen with width of approximately $\sqrt{\varepsilon}$, Heisenberg's uncertainty relation does *not* pose a problem with their propagation. One way to see this is to scale out all the factors of $\varepsilon$ in (6) with Hamiltonian (5). Thus we rescale time by $\varepsilon$ and space by $\varepsilon^2$ and end up with the adiabatic Schrödinger equation $i\partial_t \psi(R) = (-\frac{1}{2}\partial_R^2 \psi(R) + V_0^\pm(R/\varepsilon))\psi(R)$, with initial condition $\psi_{0,j}^\pm(R/\varepsilon)$. In the new scale, each slice has a width of order one, speed of order one, and needs to be propagated until it has travelled a small distance of order one. So, we can expect that no serious broadening of the wave packet takes place. The only precaution we need to take is that when the $g_j$ have a relatively sharp cutoff, we create spurious momenta originating from the steep areas of the sliced wave packets $\psi_{0,j}^+$. But these momenta are very large and thus far away from the mean momentum of the incoming wave packet $\psi_0^j$. We can therefore remove their effect after applying formula (16) and resummation of the slices simply by performing a momentum cutoff that removes momenta that are too far away from the one dictated by energy conservation. In the example of NaI, 30 slices and a cutoff procedure produced excellent agreement with exact calculations.

Let us finally remark that although equation (16) was derived by switching to the time scale $\hbar/\varepsilon$, i.e. by solving (6) instead of (4), the formula itself is instantaneous in time.

## III. SYSTEM AND NUMERICAL DETAILS

As an example, we treat the paradigmatic photo-dissociation of NaI[15]. The initial wave packet is generated by a modulated pump pulse, and then travels towards the avoided crossing. The description of the pump

TABLE I. Parameters for the potential energy surfaces of NaI (taken from Ref. 16).

| Ionic | | Neutral | | Coupling | |
|---|---|---|---|---|---|
| $A_2$ [eV] | 2760 | $A_1$[eV] | 0.813 | $A_{12}$[eV] | 0.055 |
| $B_2$ [eV$^{1/8}$ Å] | 2.389 | $\beta_1$ [Å$^{-1}$] | 4.08 | $\beta_{12}$ [Å$^{-2}$] | 0.6931 |
| $C_2$ [eV Å$^6$] | 11.3 | $R_0$[Å] | 2.67 | $R_x$[Å] | 6.93 |
| $\lambda^+$[Å$^3$] | 0.408 | | | | |
| $\lambda^-$[Å$^3$] | 6.431 | | | | |
| $\rho$[Å] | 0.3489 | | | | |
| $\Delta E_0$ [eV] | 0.2075 | | | | |

pulse as well as the potential energy surfaces are taken from the work of Engel and Metiu[16]. The only difference is that we will work in the adiabatic representation, while Engel and Metiu use the diabatic one for constructing the initial conditions. However, they also use a rapidly decaying off-diagonal element in the diabatic representation, and so the two representations coincide where the initial wave packet is created. We will always use [Å] as the unit of length and [eV] as the unit of energy.

The Hamiltonian of the model is given by (1), where $|1\rangle$ is the neutral electronic diabatic state, and $|2\rangle$ is the ionic state. Engel and Metiu use the ionic potential

$$V_2(R) := V_{22}(R) = (A_2 + (B_2/R)^8)\, e^{-R/\rho} - e^2/R$$
$$-e^2(\lambda^+ - \lambda^-)/2R^4 - C_2/R^6$$
$$-2e^2\lambda^+\lambda^-/R^7 + \Delta E_0 \qquad (22)$$

given in Ref. 17, and the neutral potential

$$V_1(R) := V_{11}(R) = A_1 \exp(-\beta_1(R - R_0)) \qquad (23)$$

from Ref. 18. They choose the diabatic coupling term as

$$V_{12}(R) = V_{21}(R) = A_{12} \exp(-\beta_{12}(R - R_x)^2). \qquad (24)$$

The constants in the above potentials are given in Table III and the potentials, along with the coupling function, are shown in Figure 2.

Since we need to work with the adiabatic energy surfaces instead of the diabatic ones, we compute the former from the latter by the formulas

$$V_0^\pm(R) = \pm\rho(R) + d(R)$$

with

$$\rho = \sqrt{(V_{11} - V_{22})^2 + V_{12}^2}, \quad d = \tfrac{1}{2}(V_{11} + V_{22}).$$

Note also that we obtain $R_c = 7.02$Å for the location of the avoided crossing in the adiabatic representation, which is slightly different from $R_x$.

The atomic masses of Na and I are 23 and 127 atomic mass units, respectively, and so (2) gives $\varepsilon^2 \approx 2.147 * 10^{-4}$.

In order to create the initial state on the upper potential energy surface, the excitation via a laser pulse is
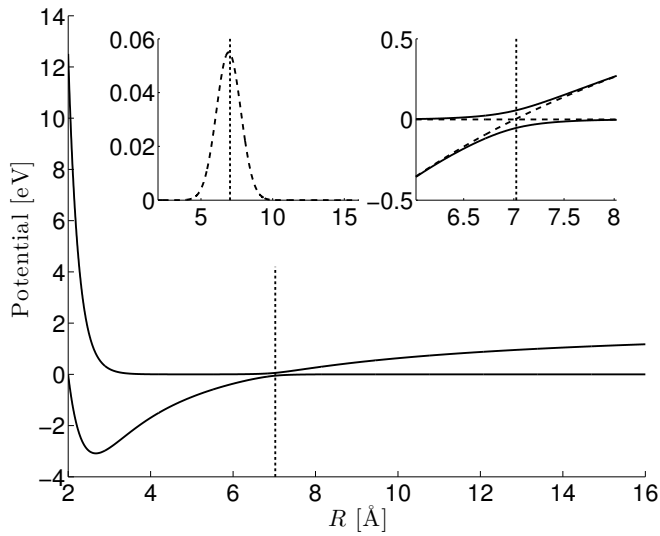
FIG. 2. Main plot: Adiabatic and diabatic potentials (solid and dashed lines, respectively), which are virtually indistinguishable on this scale. Left inset: The coupling function $V_{12}$. Right inset: zoom of the main figure around the crossing point, $R_c = 7.02$Å, marked with a vertical dotted line in all three plots.

modeled using a first-order perturbation approximation, and in the Condon approximation:[16]

$$\psi^+(t) = \frac{\mathrm{i}}{h} \int_0^t \mathrm{e}^{-(\mathrm{i}/\hbar)H^+} E(s) \exp(-\mathrm{i}\omega_v s)\phi_v \mathrm{d}s. \quad (25)$$

Here $\phi_v$ is the vibrational ground state on the lowest potential energy surface, approximated by a Gaussian, and $\omega_v$ is the corresponding vibrational frequency.

The electric field of the laser is described by

$$\boldsymbol{E}(s) = \exp(-\mathrm{i}\omega_0 s)\exp\left[-\beta(s-s_0)^2\right]. \quad (26)$$

$\omega_0$ is its peak frequency (given by $\omega_0 = 2\pi c/\lambda$, where $c$ is the speed of light and $\lambda$ is the wavelength of the laser). As in Ref. 16, we take $s_0 = 80$fs and $\beta = 1.1 \times 10^{-3}$ fs$^{-2}$ for the pulse width. This gives a full width at half maximum of 50fs.

As in Ref. 16, we assume that the laser induced fluorescence (LIF) signal is proportional to certain populations. In particular, the LIF signal is assumed to be proportional to the free Na population, which is taken to be the population of the covalent state to the right of the crossing point $R_c$,

$$P_{\mathrm{f}}(t) = \int_{R_c}^\infty |\psi_1(R,t)|^2 \mathrm{d}R. \quad (27)$$

Similarly, the bound population is taken to be

$$P_{\mathrm{b}}(t) = \int_0^{R_c} |\psi_1(R,t)|^2 \mathrm{d}R, \quad (28)$$

which measures the population of the covalent state to the left of the crossing point. It is assumed that the ionic

state population, given by

$$P_{\mathrm{i}}(t) = \int_0^\infty |\psi_2(R,t)|^2 \mathrm{d}R, \quad (29)$$

does not contribute to the LIF signal. Engel and Metiu[16] provide a critical analysis of these definitions. In addition, we introduce the adiabatic equivalents for the bound and free populations

$$\tilde{P}_{\mathrm{f}}(t) = \int_{R_c}^\infty |\psi_0^-(R,t)|^2 \mathrm{d}R \quad (30)$$

$$\tilde{P}_{\mathrm{b}}(t) = \int_0^{R_c} |\psi_0^+(R,t)|^2 \mathrm{d}R, \quad (31)$$

where $\psi_0^+$ and $\psi_0^-$ are the upper and lower adiabatic populations, respectively. Finally, we define the optimal superadiabatic free population

$$\tilde{P}_{\mathrm{f,sup}}(t) = \int_{R_c}^\infty |\psi^-(R,t)|^2 \,\mathrm{d}R, \quad (32)$$

where $\psi^-(R,t)$ is computed through formula (16). Since the coupling $V_{12}$ is localized around $R_x$, the definitions of $P_{\mathrm{f/b}}$ and $\tilde{P}_{\mathrm{f/b}}$ agree except when the wave packet is in the crossing region. By superadiabatic theory, $\tilde{P}_{\mathrm{f,sup}}(t)$ and $\tilde{P}_{\mathrm{f/b}}$ agree except when the wave packet is fairly close to the crossing region, independently of the shape of $V_{12}$. We will see later that for understanding the time evolution of the free population, the adiabatic is better than the diabatic one, and the optimal superadiabatic one is the best.

The wave packet generated by (25) turns out to be rather broad when arriving at the crossing point $R_x$. As discussed at the end of Section II C, a slicing procedure is used to split the wave packet into localized components. As noted previously, in the present application, 30 slices have been found to be sufficient. The precise nature of the slicing procedure is not important, as the quality of our results is very robust under reasonable changes of the slicing method.

## IV. RESULTS

### A. Wave packet motion and non-adiabatic transitions

In Figure 3 we show the motions of the expectation values $\langle R \rangle$ for the various wave packets involved. The wave packet generated by the modulated laser pulse (25) travels along the upper adiabatic surface until it reaches the point $R_c$ where the avoided crossing is located. Here, a wave packet appears on the lower adiabatic surface and travels outward. The original wave packet continues to evolve, and after being reflected on the right hand side slope of the potential energy surface of the excited electronic state (see Figure 2), it returns to $R_c$, where a further transmitted wave packet is spawned. Both wave
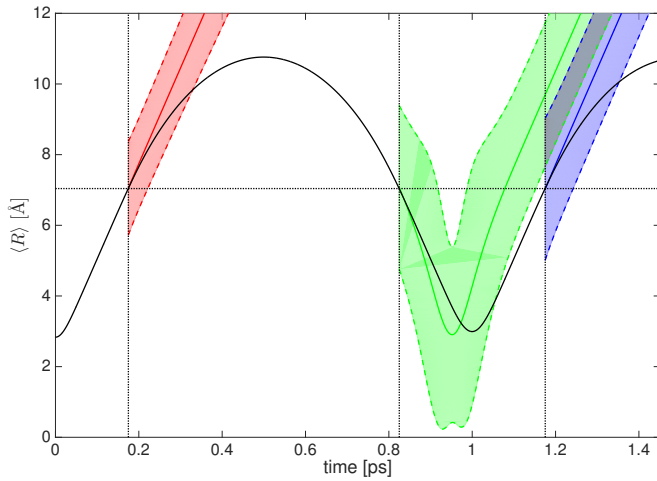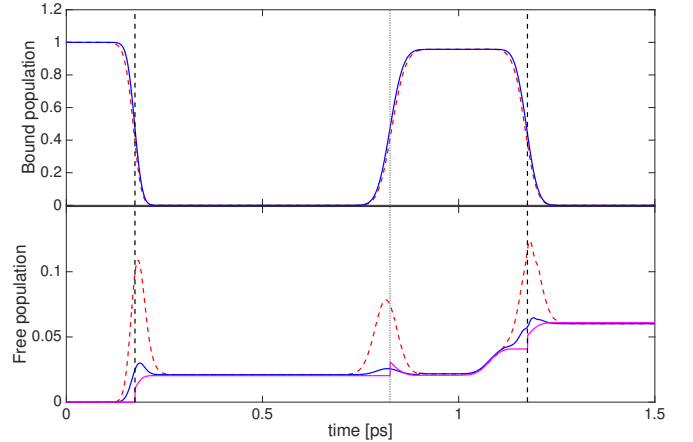
FIG. 3. In black, the expectation values $\langle R \rangle$ of the wave packet $\psi_0^+$ as a function of time. Transmitted wave packets are created each time the center of mass crosses $R_c = 7.02\mathring{A}$. The expectation values $\langle R \rangle$ of the first, second and third wave packet are shown with red, green and blue, solid lines respectively, as functions of time. We indicate the spatial delocalization of the transmitted wave packets by shading within 3 standard deviations of the mean. Note the grey area denotes the area of significant overlap of the second and third transmitted wave packets. Dotted black lines denote $R_c$ and the transmission times.



FIG. 4. Bound (top plot) and free (bottom plot) populations for the diabatic (red, dashed) and adiabatic (blue, solid) representations, as defined in (27), (28), (30) and (31), for $\lambda = 328$nm. The purple line shows the superadiabatic free population as defined in (32), and generated by instantaneously creating a wave packet according to formula (15), when the center of $\psi_0^+$ is at $R_c$.

packets are then reflected at the left hand side slope of their respective adiabatic energy surface, and return to $R_c$ at roughly the same time. A third transmitted wave packet is spawned, and creates interference effects with the second one.

Figure 4 complements Figure 3 by showing the time evolution of the populations during the first three visits of the wave packet $\psi^+(t)$ to the avoided crossing. While the diabatic and adiabatic curves for the bound populations are almost indistinguishable, the relative size difference is significant for the free population. The free population defined via the diabatic representation (Eq. (27)) shows a large spurious maximum whenever the wave packet reaches the avoided crossing. This signifies that near the crossing region, or more generally whenever it does not agree with the adiabatic representation, the diabatic representation is physically inadequate. In the adiabatic representation (blue line), the spurious build-up of the transmitted wave packet is already much weaker. It is only about 30% larger than the true transmitted wave packet for the first crossing. This is an indication that the adiabatic representation is rather close to the optimal superadiabatic representation in the case NaI; in this system, Stückelberg oscillations are present, but weak.

The purple line shows the superadiabatic free population (Eq. (32)). The discontinuities are artifacts of creating the transmitted wave packet instantaneously via Eq. (16). The subsequent build-up in the first transition signifies that when created, the wave packet only half overlaps the region $R > R_x$ and subsequently fully

enters this region. The same effect leads to the discontinuity and subsequent die-down of the second transition: the wave packet now moves left and leaves the region $R > R_x$. In the third transition, the first (continuous) build-up of free population is due to the return of the lower (super-)adiabatic wave packet created in the second transition. A bit later, also the upper adiabatic wave packet returns to the crossing, and a third transition (again with a discontinuity) takes place. This detailed information cannot be inferred from the behavior of the adiabatic population at the third crossing. In addition, the latter is rather complicated due to delicate interference effects taking place. We thus see that the superadiabatic representation is best suited for understanding the physics of non-adiabatic transitions.

## B. Transmitted wave packet at the first crossing

Figure 5 shows the absolute value and phase of the transmitted wave packet for the first transition with $\lambda = 328$nm. We plot the wave packets at the crossing point, i.e. we compare the results of (15) at $t = t_c$ with the wave packet obtained from running the full, coupled dynamics until the transmitted wave packet is well clear of the crossing region (in the scattering regime) and then evolving the transmitted wave packet back to the crossing point under the Born-Oppenheimer approximation. This is equivalent to evolving the results of (15) into the scattering regime, but results in a less-rapidly oscillating phase in momentum space. We plot our results in the momentum representation in order to highlight the change of shape that the wave packet $\psi_0^+$ (shown in the inset in momentum representation) undergoes when making the transition: while the original wave packet has a rather fat

FIG. 5. Comparison between the result of (15) ($\widehat{\psi^-}$, solid lines) and transmitted wave packet from the full, coupled dynamics ($\widehat{\phi^-}$, dotted lines) at the crossing point for $\lambda = 328$nm in momentum representation. Top plot shows the absolute values of the transmitted wave packets in the top panel, and the absolute error in the bottom panel. Bottom plot shows the phase and phase error in the top and bottom panels, respectively. Note that different scales are used to depict the values and their errors. The inset shows the wave packet on the upper potential energy surface at the crossing point.
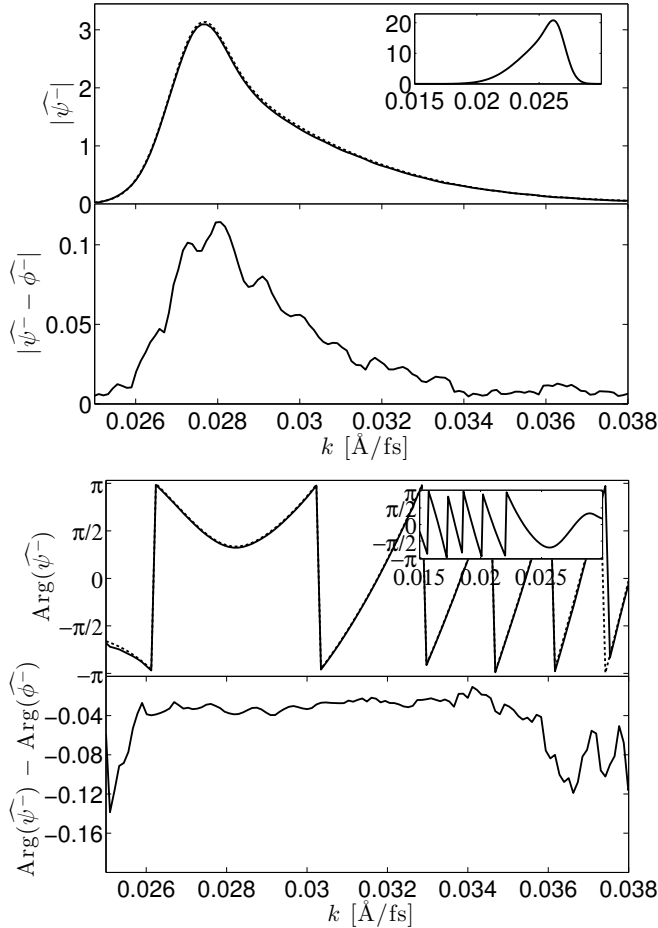


tail of low momenta, these slow parts of the wave packet make much smaller non-adiabatic transitions than the fast ones, and so the transmitted wave packet has instead a rather fat tail of high momenta. Note also that neither of the wave functions is particularly well approximated by a Gaussian. Also, the phase of both wave packets is clearly rather non-trivial. Nevertheless, formula (16) gets it right to very high accuracy.

The $L^2$ relative error between the results of (15) and the exact calculation is 0.0371 for $\lambda =$328nm. We also did the calculations for other wavelengths of the pump pulse and found that the errors for $\lambda =$300 and 310nm are 0.0240 and 0.0238, respectively.

## C. Combined transmitted wave packets at the second and third crossing

We now consider the transmitted wave packet at the avoided crossing point $R_c$ at the time $t = 1.18$ ps when the upper adiabatic wave packet $\psi^+$ reaches $R_c$ for the third time (compare Figure 3). The wave packet created by the first visit of $\psi^+$ to $R_c$ has long disappeared into the scattering regime, but the wave packet created at the second transition now comes back and interferes with the one instantaneously created at the third transition.

Figure 6 shows the absolute value of the result of this interference. The black dotted line is the exact solution, computed by the same methodology as for Figure 5. The blue line is the result of applying our algorithm based on (15) at the second and third transition time, and adding the result of the third transition to the time-evolved result of the second. The resulting error is small (7%). Using the approximate form (21) instead of (16) for calculating the transmitted wave packet results in a similar error (6%, red line). This shows that the approximation of very small $\delta$ is well justified for NaI. Note that the slightly smaller error in the second case is a result of a smaller 'global' error; the result of (15) is more accurate where the wave packet is large. The green line, however, indicates what happens when we do not take the factor $k/|k|$ into account that arises in the limit of small $\delta$ from the non-trivial prefactor $(v + k)/2|v|$ found in formula (16): then the incorrect interference effects lead to a prediction that has nothing to do with the true wave packet. This pre-factor follows from the optimal superadiabatic theory[3] and cannot be guessed or obtained by any other means that we know of. In particular, it goes beyond the pre-factors obtained in semiclassical adiabatic theory[1,19] which do not depend on momentum and do not carry a sign.

## D. Effect of various approximations on the accuracy

Towards the end of Section II, we discussed several approximations to formula (16). Since some of them (in particular the approximate calculation of $\tau_c$) may be necessary in cases where we do not have full information about the adiabatic potential energy surfaces, it is interesting to investigate their effect on the quality of our algorithm. Here we include a systematic case study of various combinations of:
(A1) Replacing the non-trivial prefactor $(v + k)/(2|v|)$ with $k/|k| = \pm1$;
(A2) Replacing $\tau_c$ with the approximation (20);
(A3) Replacing $|k - v|$ with its leading order expansion around $\delta = 0$, i.e. $2\delta/|k|$.
Using or not using each of these approximations leads to 8 different expressions for the transmitted wave packet, ranging between the full formula (15) and the Landau-Zener type formula (21). The $L^2$ and relative errors for each of these approximations (compared to the full for-

FIG. 6. Combined transmitted wave packets for second and third transitions for $\lambda = 328$nm, at the third transition time. Note the relatively good agreement between the exact solution (black, dotted), the result of (15) (blue, solid) and (21) (red, short dashes). In contrast, not including the correct prefactor in the LZ formula results in a wave packet with significant errors (green, dash-dotted).
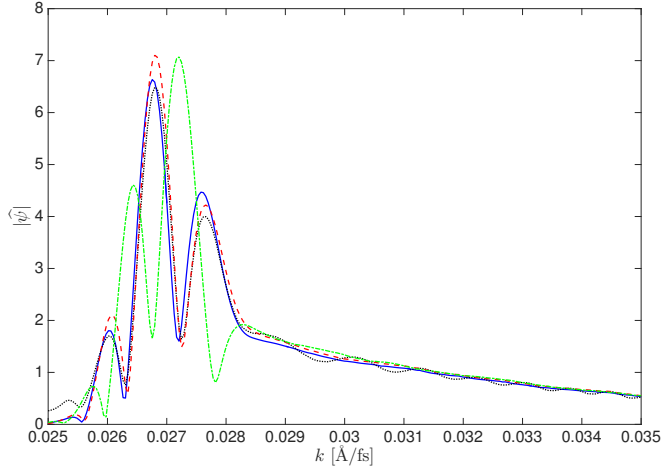


TABLE II. Error between the wave packet given by (15) with various approximations and the exact transmitted wave packet for $\lambda = 328$nm.

| | A1 | A2 | A3 | $L^2$ error | relative error to (15) |
|---|---|---|---|---|---|
| (15) | × | × | × | 0.0371 | 1 |
| | ✓ | × | × | 0.0625 | 1.69 |
| | × | ✓ | × | 0.1257 | 3.39 |
| | × | × | ✓ | 0.0665 | 1.79 |
| | ✓ | ✓ | × | 0.1286 | 3.47 |
| | ✓ | × | ✓ | 0.0401 | 1.09 |
| | × | ✓ | ✓ | 0.1494 | 4.03 |
| (21) | ✓ | ✓ | ✓ | 0.1320 | 3.56 |

mula (15)) are given in Table II for $\lambda = 328$nm. The results for $\lambda = 300$nm and $\lambda = 310$nm show a similar pattern; the $L^2$ errors are 0.0240 and 0.0238, respectively for the full formula, whilst the errors when using the Landau-Zener approximation are 0.096 and 0.104, respectively. Thus while the error of about 10% obtained by using the Landau-Zener type formula (21) is still acceptable, it is three times larger than the error we get by using the full superadiabatic formula (16).

## V. CONCLUDING REMARKS

Optimal superadiabatic representations provide an interesting framework for the description of non-adiabatic transitions at avoided crossings. They lead to monotone build up of populations over time, without spurious populations (Stückelberg oscillations) appearing at the time of the transition. Formula (15) provides a very accurate prediction of the superadiabatic transmitted wave packet, which agrees with the adiabatic one away from the crossing region. This has been verified in the example of NaI, where in particular it has been shown that even interference effects at multiple transitions are correctly predicted. The algorithm based on superadiabatic representations can thus provide an inexpensive and accurate way to predict transitions at avoided crossings, using only local information on the adiabatic electronic energies.

The present superadiabatic approach describes a non-adiabatic transition as an instantaneous transfer process, correctly accounts for phases and interference effects, and rests on a solid mathematical basis. It therefore could provide an interesting starting point for the development of semi-classical surface hopping approaches. The connection to the Landau-Zener based surface hopping approach of Belyaev, Lasser, and Trigila[14], which has been successfully applied to study the non-adiabatic dynamics of $NH_3^+$[20], was outlined. However, the work of Belyaev et al. is restricted to quasi-classical trajectories. It might interesting to combine the superadiabatic description of non-adiabatic transitions with, e.g., the semi-classical initial value[21] representation. It could provide an alternative to the classical electron analog or mapping approach[22,23] frequently used to describe multi-state dynamics in this framework.

[1]M. Berry, "Histories of adiabatic quantum transitions," P Roy Soc Lond A Mat **429**, 61–72 (1990).

[2]V. Betz, B. D. Goddard, and S. Teufel, "Superadiabatic transitions in quantum molecular dynamics," Proceedings of the Royal Society A: Mathematical, Physical and Engineering Sciences **465**, 3553–3580 (2009).

[3]V. Betz and B. D. Goddard, "Accurate prediction of nonadiabatic transitions through avoided crossings," Physical review letters **103**, 213001 (2009).

[4]V. Betz and B. D. Goddard, "Nonadiabatic transitions through tilted avoided crossings," SIAM Journal on Scientific Computing **33**, 2247–2276 (2011).

[5]D. Zener, "Non-adiabatic crossings of energy levels," Proc. Roy. Soc. London **137**, 696–702 (1932).

[6]A. Joye, G. Mileti, and C. Pfister, "Interferences in adiabatic transitions probabilities mediated by Stokes lines," Physical Review A **44**, 4280–4295 (1991).

[7]S. Teufel, *Adiabatic perturbation theory in quantum dynamics*, Lecture Notes in Mathematics, Vol. 1821 (Springer-Verlag, Berlin, 2003) pp. vi+236.

[8]C. A. Mead, "Conditions for the definition of a strictly diabatic electronic basis for molecular systems," The Journal of Chemical Physics **77**, 6090 (1982).

[9]U. Manthe and H. Köppel, "Dynamics on potential energy sur-

faces with a conical intersection: adiabatic, intermediate, and diabatic behavior," J. Chem. Phys. **93**, 1658–1669 (1990).

[10]M. Berry and R. Lim, "Universal transition prefactors derived by superadiabatic renormalization," J Phys A-Math Gen **26**, 4737–4747 (1993).

[11]R. Dingle, *Asymptotic expansions: their derivation and interpretation* (Academic Press, New York, London, 1973).

[12]V. Betz and S. Teufel, "Precise coupling terms in adiabatic quantum evolution: the generic case," Comm. Math. Phys. **260**, 481–509 (2005).

[13]M. Berry, "Universal oscillations of high derivatives," Proceedings of the Royal Society A: Mathematical, Physical and Engineering Sciences **461**, 1735–1751 (2005).

[14]A. Belyaev, C. Lasser, and G. Trigila, "Landau-Zener type surface hopping algorithms," J. Chem. Phys. **140**, 224108 (2014).

[15]A. H. Zewail, *Femtochemistry: Ultrafast Dynamics of the chemical bond* (World Scientific, New York, 1994).

[16]V. Engel and H. Metiu, "A quantum mechanical study of predissociation dynamics of NaI excited by a femtosecond laser pulse," The Journal of Chemical Physics **90**, 6116–6128 (1989).

[17]M. B. Faist, "Collisional ionization and elastic scattering in alkali–halogen atom collisions," The Journal of Chemical Physics **64**, 2953 (1976).

[18]N. J. A. van Veen, M. S. De Vries, J. D. Sokol, T. Baller, and A. E. de Vries, "Wavelength dependence of photofragmentation processes of the first excited states of Na and K halides," Chemical Physics **56**, 81–90 (1981).

[19]A. Joye, H. Kunz, and C. E. Pfister, "Exponential decay and geometric aspect of transition probabilities in the adiabatic limit," Annals of Physics **208**, 299–332 (1991).

[20]A. K. Belyaev, W. Domcke, C. Lasser, and G. Trigila, "Nonadiabatic nuclear dynamics of the ammonia cation studied by surface hopping classical trajectory calculations," J. Chem. Phys. **142**, 104307 (2015).

[21]W. H. Miller, "The semiclassical initial value representation: A potentially practical way for adding quantum effects to classical molecular dynamics simulations," J. Phys. Chem. A **105**, 2942–2955 (2001).

[22]H. D. Meyer and W. H. Miller, J. Chem. Phys. **70**, 3214 (1979).

[23]G. Stock and M. Thoss, Phys. Rev. Lett. **78**, 578 (1997).